

Natalia Dubrovina⁽¹⁾, Elena Durán-Valdeiglesias⁽¹⁾, H  l  ne Debr  geas⁽¹⁾, Ricardo Rosales⁽²⁾, Fran  ois Lelarge⁽¹⁾, Romain Brenot⁽³⁾

⁽³⁾ Huawei Technologies, 92100 Boulogne Billancourt, Paris, France

Laser and modulator phosphorus-based multi-quantum wells (MQWs) structures are grown by Gas Source Molecular Beam Epitaxy (GSMBE), with butt-joint technology, enabling to

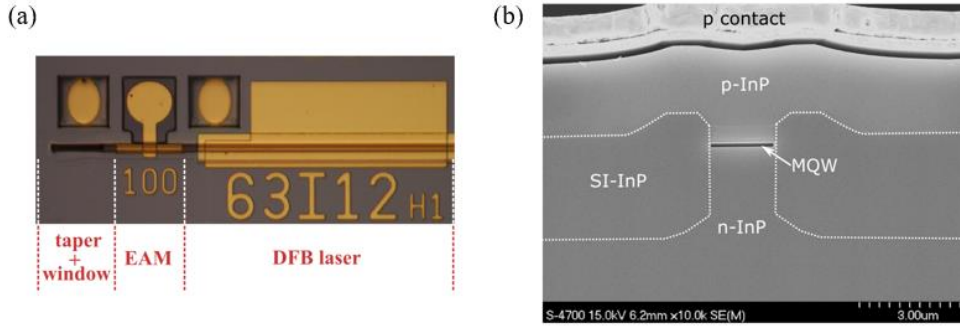


Fig. 1: (a) Optical microscope image of a chip; (b) SEM image of chip cross section.

independently tune both structures (MQW stack, bandgap energy, doping profile). To form the waveguide, we use a semi-insulated buried heterostructures (SIBH) technology, which is well known for providing high modulation speed, efficient thermal dissipation, low series resistance, and a quasi-circular optical mode.

The laser section MQW stack, doping profile and DFB grating strength are optimized to deliver high output power. The modulator MQW stack is designed to provide 15% optical confinement in the MQW, which, in our case, ensures sufficient extinction. Besides, the modulator section length is chosen to be 100 μm that seems to be a near-optimal length for 50Gb/s operation: it provides high-enough electro-optical bandwidth, and it favours low modulator saturation level, when correct laser-modulator detuning $\Delta\lambda$ is applied.

The determination of a correct laser-modulator detuning $\Delta\lambda$ appears to be a critical point for PON application. A large $\Delta\lambda$ reduces the insertion losses and prevents modulator saturation as a large electrical field has to be applied in the QWs. However, increasing $\Delta\lambda$ leads to the requirement of using higher peak-to-peak modulation voltage (V_{pp}) in order to achieve necessary level of ER. To assist low V_{pp} even at large $\Delta\lambda$ the EAM section must provide steep extinction curve.

Therefore, our EAM section, material wise, is carefully designed to obtain the optimum

performance trade-off. For instance, our modulator MQW stack is tailored to minimize the thickness of the undoped material for the purpose of increasing electrical field applied to MQW for a given voltage between EAM electrodes. Also, the top p-cladding layers are grown by GSMBE instead of the more usual Metal-Organic Vapor Phase Epitaxy (MOVPE). In GSMBE Zinc dopant is replaced by Beryllium dopant, which exhibits much less diffusion into the underneath layers. Thus, the modulator active zone remains perfectly undoped leading to a more efficient and homogeneous application of the electrical field over the MQW region.

EML performances

Different DFB gratings have been defined on the same wafer using electron-beam lithography to cover the two 50G-PON downstream wavelengths. A fine scan around central wavelengths (1342nm and 1358nm) allows to determine the optimum laser-modulator detuning $\Delta\lambda$ for the PON application. The full wavelength span is more than 20nm.

Fig. 2 presents static performances of fabricated EMLs when chip temperature is 45°C. Fig. 2(a) shows the optical spectra of ten selected EMLs. The side mode suppression ratio remains beyond 40dB even at high DFB injection currents. All studied chips (covering full studied

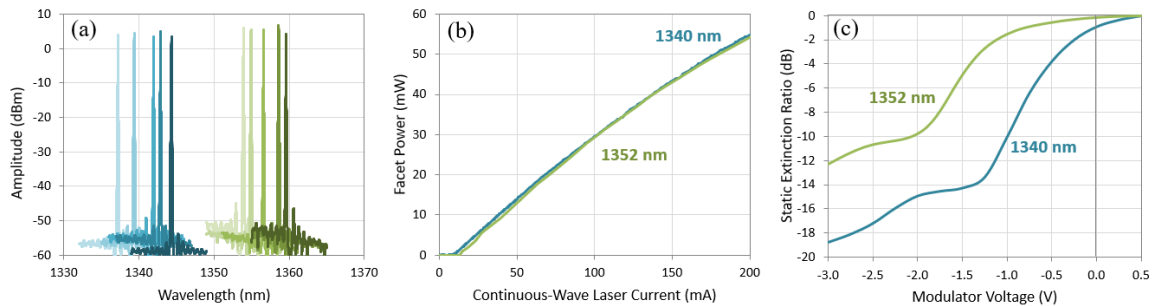


Fig. 2: Static performance at 45°C chip temperature: (a) optical spectra for different detunings $\Delta\lambda$; (b) output facet power versus laser current (continuous wave), EAM section is not connected; (c) static extinction ratio of 100 μm EAM section for standard and increased $\Delta\lambda$, laser current is 150mA.

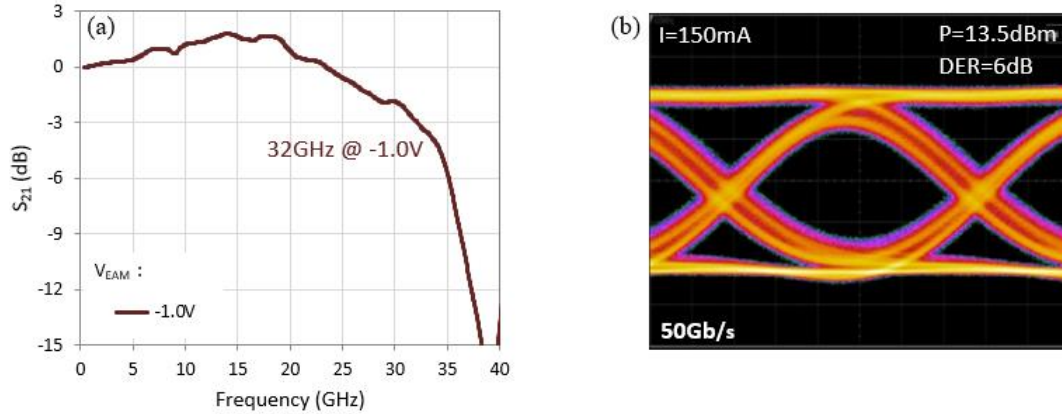


Fig. 3: Dynamic characteristics of a device at 45°C chip temperature: (a) S21 curve at -1V EAM bias and laser current 150mA; (b) 1352nm EML 50 Gb/s NRZ eye diagram for laser current 150 mA.

wavelength range) possess very similar light-current (LI) characteristics: the threshold current is below 20mA, and the output facet power is ~44mW at 150 mA. As an example, Fig. 2(b) illustrates two LI curves for chips lasing at 1340nm and 1352nm. Fig. 2(c) shows the modulator static ER. Introduced laser emission at 1340nm corresponds to the typical value of $\Delta\lambda$ that is used for our standard EML design, and it is characterised by very low (about -1dB) insertion loss at 0V and steep extinction of 14dB at -1.3V. This design allows to have high output power and low peak-to-peak modulation voltage V_{pp} . Although to reach record high output power of more than 12dBm the laser current should be increased, which may lead to the modulator saturation, when photogenerated holes accumulate in the MQW and screen the electrical field. Such field screening, in its turn, contributes to a closure of the eye diagram. This effect may be delayed when increasing $\Delta\lambda$ by 12nm (1352nm laser emission wavelength). In the case of larger $\Delta\lambda$ the extinction curve shifts to the left towards more negative voltages. Usually, this will lead to significant increment of V_{pp} value and/or ER degradation. Nevertheless, thanks to our design aiming at maximizing voltage efficiency on the modulator MQW, the ER curve remains quite steep and still provides about 10dB extinction at -2V.

The EML emitting at 1352nm and offering optimum detuning $\Delta\lambda$ was mounted on a carrier with 50Ω resistance parallel to EAM for HF matching purposes. Fig. 3(a) reports the 3dB optical bandwidth of 32GHz when the EAM bias voltage is set to -1.0V. The eye diagram for NRZ 50Gb/s presented on the Fig. 3(b) is measured at 45°C chip temperature and laser current of 150mA, without the use of any digital signal processing (DSP). The modulator voltage is applied via a bias T, added with an amplified modulation, with an estimated amplitude V_{pp}

around 2.5V. In these conditions we obtain an outstanding >13dBm average output facet power, without any saturation of the EAM section and a large 6dB dynamic ER.

Conclusions

We have presented EMLs emitting in the range from 1340nm to 1360nm for 50G-PON applications. By optimizing the modulator design and the fabrication technology we achieve increment of voltage application efficiency on the MQW. Choosing an increased laser-modulator detuning $\Delta\lambda$ we have demonstrated a record facet modulated output power of >13dBm and dynamic ER of 6dB at 50Gb/s NRZ. This EML design may enable the use of unamplified transmitters with a small footprint and low power consumption for meeting the high loss budget requirements in 50G-PON.

Our design and fabrication rules may be also expanded to other wavelength ranges. For example, to the band C where they can be applied to 1577nm high power EMLs.

References

- [1] "Physical Layer Specifications and Management Parameters for 25 Gb/s and 50 Gb/s Passive Optical Networks," IEEE 802.3ca-2020.
- [2] "50-Gigabit-capable passive optical networks (50G-PON) - Physical media dependent (PMD) layer specification," IUT-T G.9804.3.
- [3] R. Rosales, I. Cano, D. Nasset, Y. Zhicheng, R. Brenot, N. Dubrovina, E. Durán-Valdeiglesias, H. Debrégeas, D. Carrara and F. Lelarge, "First Demonstration of an E2 Class Downstream Link for 50Gb/s PON at 1342nm," 2020 European Conference on Optical Communications (ECOC), 2020, pp. 1-4. DOI: [10.1109/ECOC48923.2020.9333394](https://doi.org/10.1109/ECOC48923.2020.9333394)
- [4] I. Cano, D. Nasset and R. Brenot, "25-Gb/s Laser Modulated EML With High Output Power," in IEEE Photonics Technology Letters, vol. 32, no. 8, pp. 489-491, 15 April 15, 2020. DOI: [10.1109/LPT.2020.2980903](https://doi.org/10.1109/LPT.2020.2980903)

- [5] T. Shindo, N. Fujiwara, S. Kanazawa, M. Nada, Y. Nakanishi, Y. Yoshimatsu, A. Kanda, M. Chen, Y. Ohiso, K. Sano and H. Matsuzaki, "High Power and High Speed SOA Assisted Extended Reach EADFB Laser (AXEL) for 53-Gbaud PAM4 Fiber-Amplifier-Less 60-km Optical Link," in *Journal of Lightwave Technology*, vol. 38, no. 11, pp. 2984-2991, 1 June1, 2020.
DOI: [10.1109/JLT.2020.2974511](https://doi.org/10.1109/JLT.2020.2974511)
- [6] X. Dai, H. Debrégeas, G. Da Rold, D. Carrara, K. Louarn, E. Durán-Valdeiglesias and F. Lelarge, "Versatile Externally Modulated Lasers Technology for Multiple Telecommunication Applications," in *IEEE Journal of Selected Topics in Quantum Electronics*, vol. 27, no. 3, pp. 1-12, May-June 2021, Art no. 3400412.
DOI: [10.1109/JSTQE.2020.3029394](https://doi.org/10.1109/JSTQE.2020.3029394)